

Pairing gaps and Fermi energies at scission for ^{296}Lv alpha-decay

M. Mirea

Horia Hulubei National Institute for Physics and Nuclear Engineering, P.O. Box MG-G, Bucharest, Romania

The pairing corrections, the single particle occupation numbers, are investigated within density-dependent delta interaction formalism for pairing residual interactions. The potential barrier is computed in the framework of the macroscopic-microscopic model. The microscopic part is based on the Woods-Saxon two center shell model. The α -decay of a superheavy element is treated, by paying a special attention to the region of the scission configurations. The sequence of nuclear shapes follows the superasymmetric fission path for alpha decay. It was found that the pairing gaps of the states that reach asymptotically the potential well of the alpha particle have large values at scission but become zero after scission. The $1s_{1/2}$ single particle levels of the nascent α particle are fully occupied while the superior levels are empties in the scission region and remains in the same states during the penetration of the Coulomb barrier. The projection of the numbers of particle on the two fragments are obtained naturally. At scission, the nascent α particle forms a very bound cluster.

INTRODUCTION

As pointed out in Ref. [1], the disentanglement of the wave functions at scission between two independent fragments is an essential ingredient for calculations of the dynamical observables that characterize the fission. The Pauli principle involves a correlation between the fission fragments even after their separation. The condition of conservation for the number of particles in the BCS theory implies the existence of only one value of the Fermi energy in the precise moment when the nucleus breaks. The total number of nucleons of the system should be equal with the sum of the occupations probabilities of the single particle states of both fragments. But, in order to have integer numbers of nucleons in each of the two partners, at least two Fermi energies are required. It is questionable when and how these two Fermi energies are created and how the nucleus shares the nucleons to obtain the final mass numbers. In order to understand this phenomenon, the gaps and the Fermi energies will be investigated at scission with the pairing density-dependent delta interaction (DDDI) formalism and with the Woods-Saxon two center shell model. The DDDI approach allows to determine a state-dependent pairing interaction while the two center shell model offers the possibility to identify the localization of the single particle states in the fission fragments. For reflection-symmetric fission, the distribution of single particle occupation probabilities is the same for the two similar single particle levels schemes of the fragments. Therefore, the numbers of nucleons should be the same in the two fission products. The problem arises when reflection-asymmetries are considered at scission. The BCS theory with a constant pairing force allows only one distribution of single particle occupation probabilities that depends on the whole nuclear structure. This distribution of occupation probabilities is constrained by the total number of nucleons and gives non-integer values of the nucleon numbers in the two partners. Therefore, the alpha-decay of a super-

heavy element considered as a superasymmetric fission process will be treated as a limiting case.

THE MACROSCOPIC-MICROSCOPIC APPROACH IN THE TWO CENTER SHELL MODEL

Microscopic approaches based on the Hartree-Fock theory or the macroscopic-microscopic method have been used in the investigation in disintegration processes. The former approach is the more fundamental way to determine the driving potential. It starts with a realistic force between nucleons and constructs an appropriate many-body equation. Surpassing huge numerical difficulties, this approach can be used now to determine the barrier in cluster decay [2] or for fission [3, 4]. However, the way in which the passage from one nucleus into two separated bodies is envisaged remains a peculiar behavior of this picture. The basic idea of the alternative more phenomenological approach is that a macroscopic model, as the liquid drop one, describes quantitatively the smooth trends of the potential energy with respect to the particle number and the deformation whereas a microscopic formalism such as the shell model describes local fluctuations. The mixed macroscopic-microscopic method should reproduce both smooth trends and local fluctuations. The reliability of the latter approach was already tested in the case of α -decay by considering the process like a superasymmetric spontaneous fission [5] process. For the microscopic part the Woods-Saxon two center shell model is used [6].

In the macroscopic-microscopic method, the whole system is characterized by some collective coordinates that determine approximately the behavior of many other intrinsic variables [7–9]. The basic ingredient in such an analysis is the shape parametrization that depends on several macroscopic degrees of freedom. The generalized coordinates associated with these degrees of freedom vary

in time leading to a split of the nuclear system in two separated fragments. The model is valid as long as the time-dependent variations of the generalized coordinates make sense.

Nuclear shape parametrization

We use an axial symmetric nuclear shape that offers the possibility to obtain a continuous transition from one initial nucleus to the separated fragments. This parametrization is obtained by smoothly joining two spheroids of semi-axis a_i and b_i ($i=1,2$) with a neck surface generated by the rotation of a circle of radius R_3 around the axis of symmetry. By imposing the condition of volume conservation we are left with five independent generalized coordinates $\{q_i\}$ ($i=1,5$) that can be associated to five degrees of freedom: the elongation $R = z_2 - z_1$ given by the distance between the centers of the spheroids; the necking parameter $C_3 = S/R_3$ related to the curvature of the neck, the eccentricities $\epsilon_i = \sqrt{1 - (b_i/a_i)^2}$ ($i=1,2$) associated with the deformations of the nascent fragments and the mass asymmetry parameter $\eta = a_1/a_2$. Alternatively, the mass asymmetry can be characterized also by the mass number of the light fragment A_2 . This number is obtained by considering that the sum of the volumes of two virtual ellipsoids characterized by the mass asymmetry parameter η and the eccentricities ϵ_i ($i=1,2$) gives the volume of the parent. The nuclear shape is displayed in Fig. 1 where the geometrical parameters could be identified.

Pairing corrections

The macroscopic deformation energy is calculated in the framework of the finite range liquid drop model [10]. A so called correction to the macroscopic value is then evaluated using the Strutinsky procedure [11]. The Strutinsky effects contain two terms: a shell correction and a pairing one. The shell corrections take into account non-uniformities in the nuclear structure as function of the deformation or the number of nucleons. No information about the pairing are given by the macroscopic energy or the shell effects. Therefore, only the pairing corrections are interesting for our treatment.

The pairing corrections in the framework of the macroscopic-microscopic model are given by the difference

$$\delta P = E_p - \tilde{E}_p \quad (1)$$

between an exact value and an averaged one. The total energy with pairing interactions can be approximated

with the relation

$$E_p = 2 \sum_k \rho_k \epsilon_k - \sum_k u_k v_k \sum_{k'} u_{k'} v_{k'} G_{kk'} - \sum_k G_{kk} v_k^4 \quad (2)$$

The energy of a system without taking into consideration the variations of occupation probabilities and for an uniform distribution of levels reads [12]

$$\tilde{E}_p = 2 \sum_{k \leq k_F} \epsilon_k - \frac{1}{2} \tilde{g}(\tilde{\lambda}) \tilde{\Delta}^2 - G \frac{N}{2} \quad (3)$$

where k_F labels the Fermi level, $\tilde{g}(\tilde{\lambda})$ is the average level density at the smoothed Fermi energy $\tilde{\lambda}$, N the number of nucleons, G is the averaged pairing interaction, and $\tilde{\Delta} = 12/A^{1/2}$ MeV is an average gap [11, 12]. It is assumed that the last two terms in the average pairing energy

$$E_a = -\frac{1}{2} \tilde{g}(\tilde{\lambda}) \tilde{\Delta}^2 - G \frac{N}{2} \quad (4)$$

with the interaction strength

$$\frac{1}{G} = \tilde{g}(\tilde{\lambda}) \ln \left(\frac{2\Omega}{2} \right) \quad (5)$$

is contained already in the liquid drop part of the total energy [13]. Therefore, a problem is raised by this average pairing energy when the nucleus is split into two fragments. The authors of Ref. [12] emphasized the fact that a double counting should be envisaged at scission that can be eliminated by considering a dependence of the pairing strength with deformation [14].

The Woods-Saxon two center shell model

The many-body wave function and the single particle energies are provided by the Woods-Saxon two-center shell model [6]. The Woods-Saxon potential, the Coulomb interaction and the spin orbit term must be diagonalized in a double center eigenvectors basis. A complete analytical eigenvectors basis can be only obtained for the semi-symmetric two-center oscillator. This potential corresponds to a shape parametrization given by two ellipsoids that possess the same semi-axis perpendicular on the axis of symmetry. The potential is

$$V_o(\rho, z) = \begin{cases} \frac{1}{2} m \omega_{z1}^2 (z - c_1)^2 + \frac{1}{2} m \omega_\rho^2, & z < 0, \\ \frac{1}{2} m \omega_{z2}^2 (z - c_2)^2 + \frac{1}{2} m \omega_\rho^2, & z \geq 0, \end{cases} \quad (6)$$

where ω denotes the stiffness of the potential along different directions as follows, $\omega_{z1} = \omega_0 \frac{R_0}{a_1}$, $\omega_{z2} = \omega_0 \frac{R_0}{a_2}$, $\omega_\rho = \omega_0 \frac{R_0}{b_1}$, $\omega_0 = 41 A_0^{-1/3}$, $R_0 = r_0 A_0^{1/3}$, in order to ensure a constant value of the potential on the surface. The origin on the z -axis is considered as the location of the plane of intersection between the two ellipsoids.

The asymmetric two center shell oscillator provides an orthogonal eigenvectors basis for only one Hermite space [15, 16]. An analytic system of eigenvectors can be obtained for V_0 by solving the Schrödinger equation:

$$\left[-\frac{\hbar^2}{2m_0}\Delta + V_o(\rho, z) \right] \Psi(\rho, z, \varphi) = E\Psi(\rho, z, \varphi) \quad (7)$$

The analytic solution of Eq. (7) is obtained using the ansatz

$$\Psi(\rho, z, \varphi) = Z(z)R(\rho)\Phi(\varphi) \quad (8)$$

with

$$\Phi_m(\varphi) = \frac{1}{\sqrt{2\pi}} \exp(im\varphi) \quad (9)$$

$$R_{nm}(\rho) = \sqrt{\frac{2n!}{(n+m)!}} \alpha_\rho \exp\left(-\frac{\alpha_\rho^2 \rho^2}{2}\right) (\alpha_\rho \rho)^m L_n^m(\alpha_\rho^2 \rho^2) \quad (10)$$

$$Z_\nu(z) = \begin{cases} C_{\nu_1} \exp\left(-\frac{\alpha_{z1}^2(z-c_1)^2}{2}\right) \mathbf{H}_{\nu_1}[-\alpha_{z1}(z+c_1)], & z < 0; \\ C_{\nu_2} \exp\left(-\frac{\alpha_{z2}^2(z-c_2)^2}{2}\right) \mathbf{H}_{\nu_2}[\alpha_{z2}(z-c_2)], & z \geq 0, \end{cases} \quad (11)$$

where $L_n^m(x)$ is the Laguerre polynomial, $\mathbf{H}_\nu(\zeta)$ is the Hermite function, $\alpha_l = (m_0\omega_l/\hbar)^{1/2}$ ($l = z_1, z_2, \rho$) are length parameters, and C_{ν_i} ($i = 1, 2$) denote the normalization constants. The quantum numbers n and m are integers while the quantum numbers ν_i along the z -axis are real and have different values for the intervals $(-\infty, 0]$ and $[0, \infty)$. Imposing conditions for the continuity of the wave function and its derivative, together with those for the stationary energy and orthonormality, the values of ν_1 , ν_2 , and of the normalization constants C_{ν_1} , and C_{ν_2} could be obtained. Details concerning these solutions and expressions for the normalization constants are found in Refs. [15, 16]. For reflection-symmetric shapes, the solutions along the z -axis are also characterized by the parity as a good quantum number. The basis (11) for the two-center oscillators can be used for various ranges of models which are more or less phenomenological ones [17–23].

In this unique Hermite space, the behavior of both fragments can be described simultaneously. The orthogonal wave functions are centered in one of the two regions in three-dimensional position space. Each wave function is analytically continued in both regions. In an intermediate situation of two partially overlapped potentials, each eigenfunction has components in the two subspaces that belong to the fragments. When the elongation R is zero, the eigenvectors basis becomes that of a single anisotropic oscillator and the Hermite function is transformed into an Hermite polynomial. When R tends to

infinity, a two oscillators eigenvectors system is obtained naturally in the same Hermite space, centered in the middle of the two fragments. Asymptotically, when the elongation tends to infinity, only one of the values ν_1 or ν_2 is transformed into an integer. The associated Hermite function becomes a Hermite polynomial with its proper normalization constant. In the same time, the normalization constant of the other Hermite function reaches a zero value. The Pauli principle is fulfilled. Even for symmetric two center potentials, only one state is simultaneously active in all the position space. Therefore, the two center shell model always provides the wave functions associated to the lower energies of the single particle states pertaining to a major quantum number N_{max} . As a consequence, molecular states formed by two fragments at scission could be precisely described. In contrast to the cluster approximations, the two-center shell model offers the opportunity to treat fission in a wide range of mass asymmetries [24, 25] and offers to opportunity to consider the alpha decay as a supersymmetric fission process [5, 26, 27].

If the wave function is located in only one of the two potential wells, it is possible to identify the single particle states that belong to each fragment at scission. The square of the single particle wave function of each state is integrated separately in the two subspaces and two probabilities are obtained. The single particle wave function is located in the well characterized by the larger probability. Such tasks were already performed [28–30] in order to estimate the partition of the excitation energy in fission processes between the two partners.

THE DENSITY-DEPENDENT DELTA INTERACTION

A simple treatment of the pairing interaction in which the major contribution to the residual interaction is coming from the nuclear surface region is given by the DDDI model [31]. The following spatial modulation of the pairing strength is postulated [32–35] as follows:

$$V_p(\vec{r}) = -V_{0p} \left[1 - \beta \left(\frac{\rho(\vec{r})}{\rho_0} \right)^\gamma \right] \quad (12)$$

The fitting parameters $\beta=1$ and $\gamma=1$ are usually considered as unity. The saturation density of the nuclear matter is $\rho_0=0.16 \text{ fm}^{-3}$, while the $\rho(r)$ is the local density. We consider here that the local nuclear density is shape dependent and its behavior can be described by a Woods-Saxon function, in accordance to the shape of the potential used. The parameters V_{0p} of the interaction (12) should be adjusted to reproduce observables. In our case, the observable is the pairing gap. Values of the model dependent strength parameters V_{0p} are deduced in several works, as for example in Ref. [33], V_{0p} being -999

MeV fm⁻³ and -1146 MeV fm⁻³ for neutrons and protons, respectively. The values deduced in our treatment are different, as it will be specified later. The calculations based on this schematic pairing interaction could be solved on a finite space of states, called active levels pairing space. This space is limited by some cutoff in the single particle energies.

For the pairing field given by formula (12), the state-dependent pairing interaction strengths G_{ij} are defined as:

$$G_{ij} = - \int V_p(\vec{r}) |\phi_i(\vec{r})|^2 |\phi_j(\vec{r})|^2 d\vec{r} \quad (13)$$

where $\phi_j(\vec{r})$ is the wave function of the state j in the position representation. The pairing state-dependent gaps resort from the BCS equations

$$\Delta_i = \frac{1}{2} \sum_j \frac{G_{ij} \Delta_j}{\sqrt{(\epsilon_j - \lambda)^2 + \Delta_j^2}} \quad (14)$$

that are correlated by the condition of a fixed number of pairs N_p in the active levels pairing space:

$$N_p = \sum_i v_i^2. \quad (15)$$

In the previous equalities, it is considered that the index i run over $2N_p$ levels around the Fermi energy. The occupation probability of the state i is

$$v_i^2 = \frac{1}{2} \left[1 - \frac{\epsilon_i - \lambda}{\sqrt{(\epsilon_i - \lambda)^2 + \Delta_i^2}} \right] \quad (16)$$

while the vacancy probability is $u_i^2 = 1 - v_i^2$. In the previous equation, λ represents the Fermi energy of the whole nuclear system. The averaged pairing energy gap of the whole system could be considered as

$$\bar{\Delta} = \frac{\sum_i u_i v_i \Delta_i}{\sum_i u_i v_i} \quad (17)$$

This definition emphasizes the importance of the single particle levels located in the vicinity of the Fermi energy because the weights $u_i v_i$ are larger in this region.

In order to determine the parameter V_{0p} of the pairing field for a given levels pairing space, we must refer to the empirical values of the pairing gaps. A reliable value for the energy gap can be obtained with the five points formula [17] that takes into account the experimental masses. Unfortunately, no enough experimental or evaluated masses are available to date [36] in the vicinities of the nuclei ²⁹⁶Lv and ²⁹²Fl. It is not possible to extract reliable empirical pairing gap values. Therefore, our estimations rely on theoretical evaluations. The theoretical tables [37] give the next values for ²⁹⁶Lv: $\Delta_p=0.66$ MeV and $\Delta_n=0.56$ MeV, where the index p or n denotes proton or neutron, respectively. For ²⁹²Fl we have

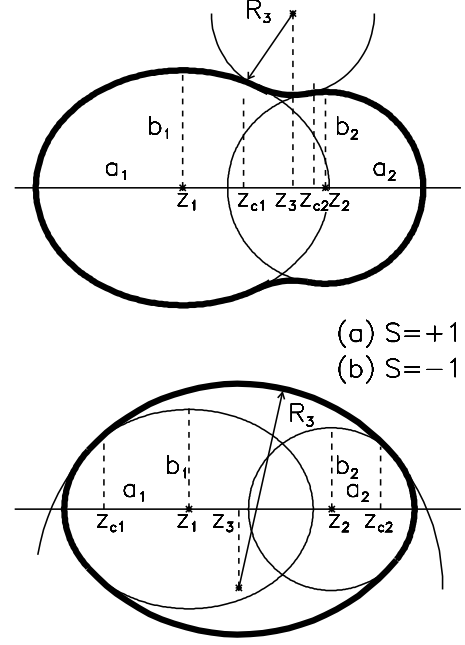


FIG. 1. Nuclear shape parametrization.

$\Delta_p=0.71$ MeV and $\Delta_n=0.60$ MeV. The ²⁹⁶Lv theoretical interaction strengths V_{0p} for the pairing matrix elements that are able to reproduce these gap values were estimated as -1448 MeV fm⁻³ and -1528 MeV fm⁻³ for neutrons and protons, respectively. In the case of the ²⁹²Fl, we obtained -1440 MeV fm⁻³ for neutrons and -1605 MeV fm⁻³ for protons. We used two active levels pairing spaces of $2N_p=190$ and $2N_p=116$ single particle levels, corresponding to the ²⁹⁶Lv numbers of neutrons and protons, respectively. It is considered that the values of the pairing strengths vary linearly from the ground state of the parent nucleus up to the scission configuration. In other words, the nascent α particle feels the pairing field of the daughter. The pairing strength spatial modulation is represented in the Fig. 2 for the touching configuration between the daughter nucleus and the α particle.

RESULTS

In our previous study, a path for the superasymmetric fission leading to alpha emission was obtained for ²⁹⁶Lv [5]. This least action path is assigned along a so called α valley in the deformation energy surface and crosses a molecular minimum. The α particle is born in this molecular minimum. The scission configuration is produced for an elongation $R \approx 10$ fm.

The single particle levels schemes along the superasymmetric fission path are displayed in Figs. 3 and 4, for

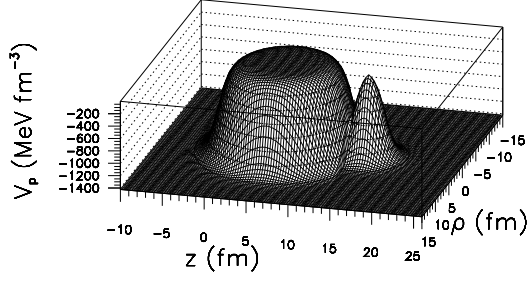


FIG. 2. The pairing strength V_p as function of the cylindrical coordinates ρ and z that characterize the shape of the nuclear system at a distance between the centers of the fragments $R=10$ fm.

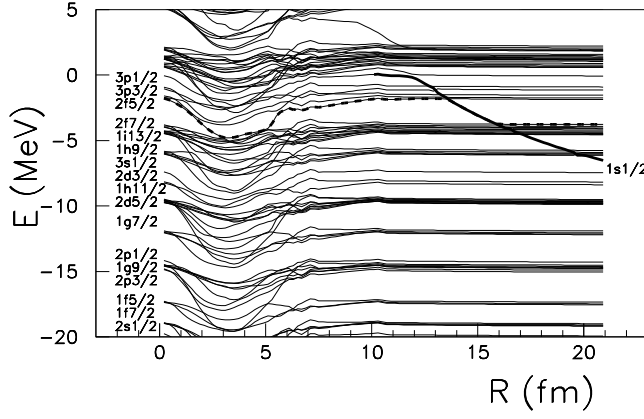


FIG. 3. Single particle level scheme for protons in the region of the Fermi energy as function of the elongation R for α -decay of ^{296}Lv . The Fermi level is plotted with a thick dashed line while the level pertaining to the alpha nucleus is plotted with thick solid lines. The orbital of the alpha nucleus is marked on the right.

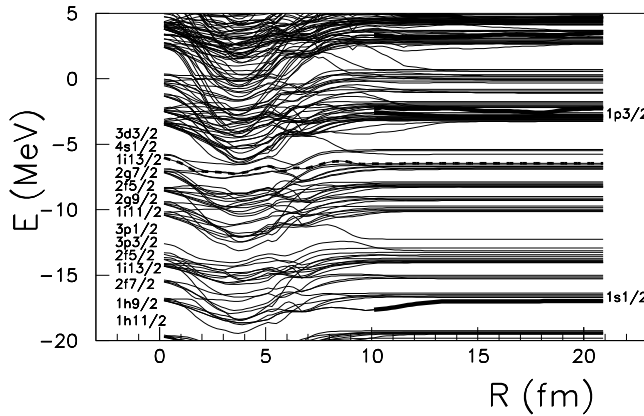


FIG. 4. Single particle level scheme for neutrons in the region of the Fermi energy as function of the elongation R for α -decay of ^{296}Lv . The Fermi level is plotted with a thick dashed line while the levels pertaining to the alpha nucleus are plotted with thick solid lines. The orbitals of the alpha nucleus are marked on the right.

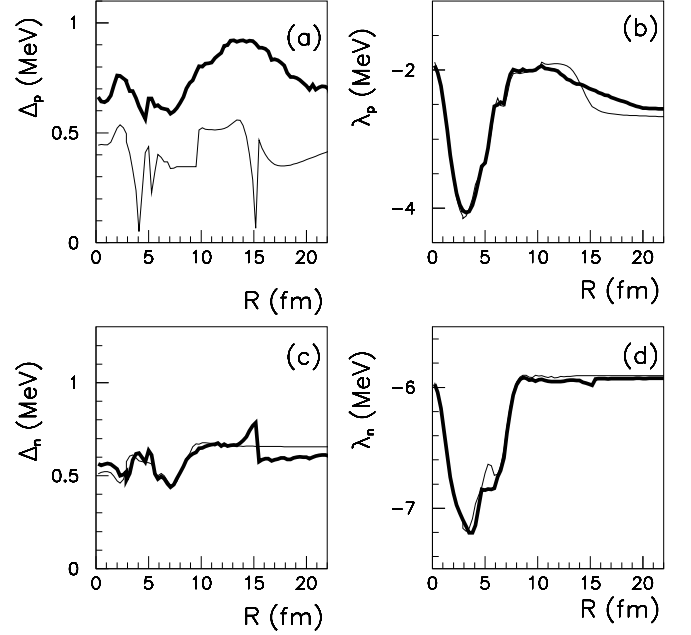


FIG. 5. Energy pairing gaps and Fermi energies. (a) The proton pairing gap Δ_p in the DDDI approach as function of the elongation R is displayed with a full thick line. The proton pairing gap for a constant strength value G is plotted with a thin line. (b) The proton Fermi energy λ_p of the whole nuclear system in the DDDI approach is plotted with a full thick line as function of the elongation R . The Fermi energy in the constant G approximation is displayed with a thin line. (c) The neutron pairing gap Δ_n in the DDDI approach as function of the elongation R is displayed with a full thick line. The proton pairing gap for a constant strength value G is plotted with a thin line. (d) The neutron Fermi energy λ_n of the whole nuclear system in the DDDI approach is plotted with a full thick line as function of the elongation R . The Fermi energy in the constant G approximation is displayed with a thin line.

protons and neutrons, respectively. An energy window around the Fermi level is selected to evidence the mean features of the process. As mentioned, close to the scission configuration the two center shell model offers the possibility to identify the single particle levels that pertain to the alpha particle. These levels are plotted with thick solid lines. Asymptotically, the model gives a superposition of both the single particle level schemes of the daughter nucleus and of the α particle. If the BCS equations with constant pairing strength G are solved in the region of separated nuclei, this superposition of single particle level schemes should be taken into consideration, no matter the affiliation of the nucleons in one of the nuclear fragments. The Fermi single particle levels are plotted with a thick dashed line in both figures. A polarization effect is clearly visible for the $1s_{1/2}$ proton single particle level associated to the α particle. The energy of this level decreases when the two nuclei

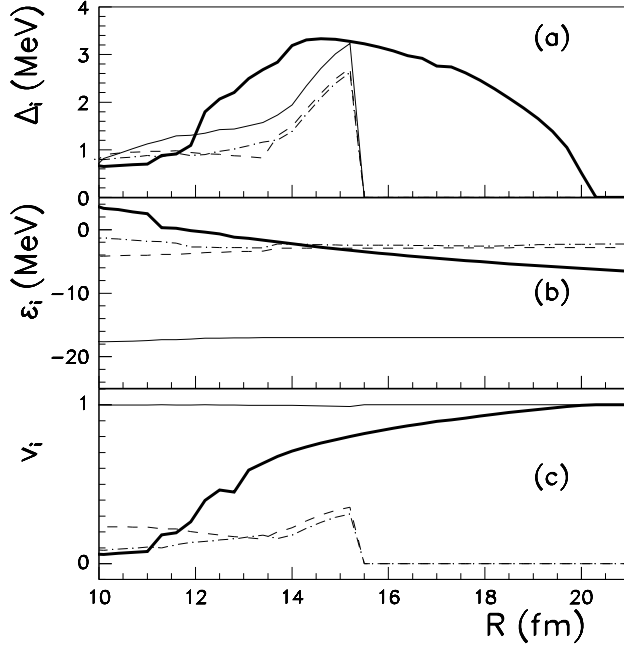


FIG. 6. (a) Values of the state-dependent pairing gap parameters Δ_i for the lower single-particles states that reach the α nucleus after the scission as function of the elongation R . The thick full line corresponds to the proton asymptotic state $1s_{1/2}$, the thin full line is for the neutron final state $1s_{1/2}$, while the dot dashed and dashed lines are associated to the two $1p_{3/2}$ neutron states. (b) Single particle energies ϵ_i for these orbital. The same line types as in the caption (a) identify the states. (c) BCS amplitudes v_i for the above mentioned states. The line types refer to the same states as in caption (a).

get away one from another. After the scission, this level crosses many shells of the daughter nucleus. The proton energies of the daughter nucleus decrease also after the scission, but with a much smaller slope.

First of all, the Fermi energies and the pairing gaps of the whole nuclear system are calculated along the supersymmetric fission trajectory in the framework of the DDDI approach and (for comparison) under the hypothesis of a constant pairing strength G . We calculated the averaged pairing gaps of the whole nuclear system with the Eq. (17). The results are displayed in Fig. 5. A thick line is used for the DDDI formalism while a thin one for the G constant approximation. Both approaches give a gross similar structure in the variation of the pairing gaps and of the Fermi energies as function of the distance between the centers of the fragments R . The values of the DDDI proton pairing Δ_p are always larger than those given by the constant G approximation. A sudden variation is obtained for the DDDI neutron pairing gap Δ_n at $R \approx 15$ fm. This variation could be understood in the following analysis of the state dependent pairing gaps. It is important to note that the average values of the gaps

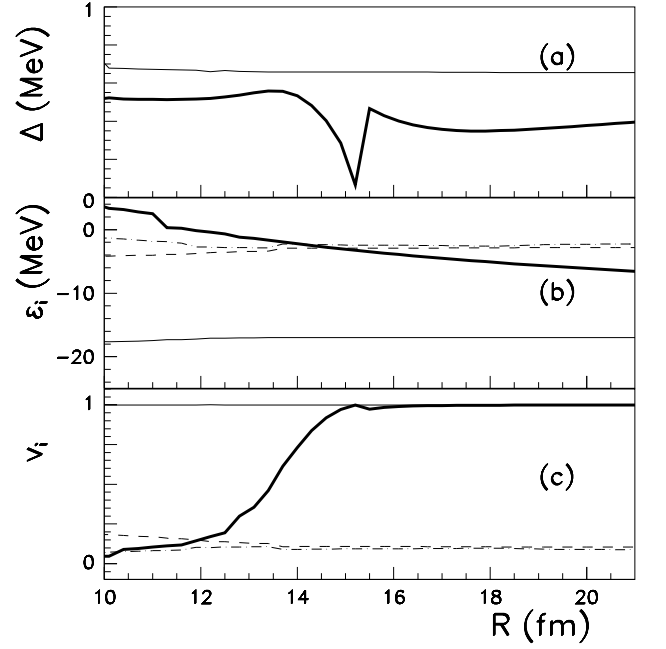


FIG. 7. (a) Values of the pairing gap parameters Δ in the BCS approximation with a constant value of the pairing interaction G . The thick line represents the pairing gap for proton while the thin line indicates the pairing gap for neutron. (b) Single particle energies ϵ_i for the orbitals that reach the alpha nucleus. The same line types as in Fig. 6 are used. (c) BCS amplitudes v_i calculated with constant pairing interaction approach. The line types refer to the same states as in caption (b).

never exceed 1 MeV for both isospins.

In Fig. 6(a), the pairing gaps Δ_i associated to the single particle states that pertain to the α potential well after the scission are plotted as function of the elongation R . For simplicity, only single particle levels with energies located in the vicinity of the Fermi energy of the compound system are displayed. In the case of proton, only the α $1s_{1/2}$ state could be selected in the given energy window. In the case of neutron, three single particle levels are identified. The energies of all these single particle levels are displayed with thick lines for proton and thin lines for neutron in Fig. 6(b). In the Fig. 6(c), the occupation amplitudes v_i of the selected single particle states are plotted. The gap associated to the neutron $1s_{1/2}$ α -state increases up to a value close to 3.5 MeV at an elongation $R \approx 14$ fm. After this distance between the centers of the nascent fragments, the gap drops to zero but the occupation amplitude reaches the value of unity. The gaps associated to the superior neutron single particle levels have a different behavior. Their gaps drop to zero at the same value of the elongation while the occupation amplitudes reach zero values. In the case of the proton $1s_{1/2}$ single particle state, the gap reaches a zero value at an elongation close to 19 fm and its occu-

pation amplitudes becomes unity. These behavior reflect the short range character of the nuclear forces and the long range character of the Coulomb interaction. After a certain distance between the two nuclei ($R \approx 10\text{-}19\text{ fm}$), the pairing interactions G_{ij} between orbitals located in different single particle potentials become zero. The connections between the pairing gaps Δ_i for single particle states located in different fragments given by the values of G_{ij} in Eqs. (14) are lost. Therefore, the pairing equations (14) are nearly transformed into two separated systems of equations, one for the daughter and another for the alpha particle, correlated only by the value of the Fermi energy λ . It was already noticed that the average values of the DDDI pairing gaps never exceed 1 MeV. In consequence, it can be assessed that the values of the pairing gaps associated to the alpha particle are always larger than those associated to the daughter nucleus in the vicinity of the scission configuration. These large values of the α energy gaps close to 3.5 MeV at scission have a particular importance for the alpha decay process. The quasiparticle energies of the alpha states are very large. That means, the quasiparticle excitations of the nascent alpha particle close to scission are strongly suppressed.

For comparison purposes, the occupation probabilities of the single particle levels were also calculated in the constant pairing interaction approach. The value of the interaction G is obtained within a normalization procedure that takes into account the density of levels at the Fermi energy and the average gap $\tilde{\Delta}$ [11]. The results are plotted in Fig. 7. The values of the gap Δ as function of the internuclear distance are displayed in the panel (a). The values of the gap parameters never reach a zero value, being the same as for all nucleons of the same specie of the whole nuclear system. A fluctuation of the proton pairing gap can be observed at $R \approx 15.2\text{ fm}$. This fluctuation reflects the crossing between the $1s_{1/2}$ single particle state of the α particle with a shell of the daughter located in the vicinity of the Fermi energy. The proton single particle level can be identified in panel (b). In panel (c) the occupation amplitudes are plotted. The amplitude of the proton state reaches the value of unity at an internuclear elongation smaller than that in the case obtained with DDDI. The lowest neutron state $1s_{1/2}$ has practically a constant occupation amplitude, slightly lower than unity. The outer neutron orbitals ($1p_{3/2}$) remain with non-zero values of their occupation amplitudes, even after the scission. That means, the emitted nucleus has a (real) number of neutrons larger than 2 in the constant G approximation.

A Fermi energy λ' for the daughter can be obtained by solving the equation for the number of particles

$$N_d = \sum_{i'} v_{i'}^2. \quad (18)$$

where it is considered that the index i' runs over $2N_{dp}$ levels for states located in the daughter well that can

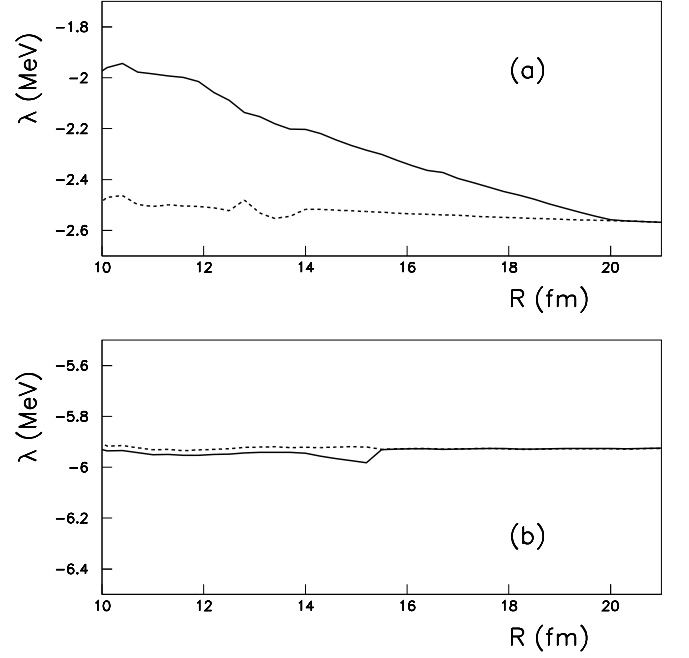


FIG. 8. The whole system Fermi energies λ for proton (a) and neutron (b) are plotted with full lines. The Fermi energies of the daughter λ' are displayed with a dashed line.

be provided by the active level pairing space. $2N_d$ is the number of nucleons of the daughter. The occupation probability of the state i' is

$$v_{i'}^2 = \frac{1}{2} \left[1 - \frac{\epsilon_{i'} - \lambda'}{\sqrt{(\epsilon_{i'} - \lambda')^2 + \Delta_{i'}^2}} \right] \quad (19)$$

Consequently, λ' is now the Fermi energy of the daughter.

In Fig. 8, the Fermi energies λ of the whole system are plotted with a full line while the dashed lines correspond to the Fermi energies of the daughter λ' . The panel (a) corresponds to proton while the (b) one to neutron. It is interesting to note that λ becomes equal to λ' asymptotically, no matter the isospin.

In Fig. 9, the pairing corrections for proton δP_p (a) and for neutron δP_n (b) are calculated with the formula (1) along the supersymmetric fission trajectory in the DDDI approach. The pairing correction formalism is not an appropriate treatment in the case of the α particle. Terms like those given by the expression (4) cannot be constructed. Therefore, the terms proportional to G_{ii} in which i denote states of the α particle were gradually suppressed after the scission in formula (1). Asymptotically, we are left with the pairing effects of the daughter. The values of the proton pairing correction δP_p exhibit a structure with a negative fluctuation at $R \approx 13\text{-}14\text{ fm}$. Usually the pairing corrections increase for low density of levels around the Fermi energy. So, this negative fluctuation reflects the fact that the single particle energy of the

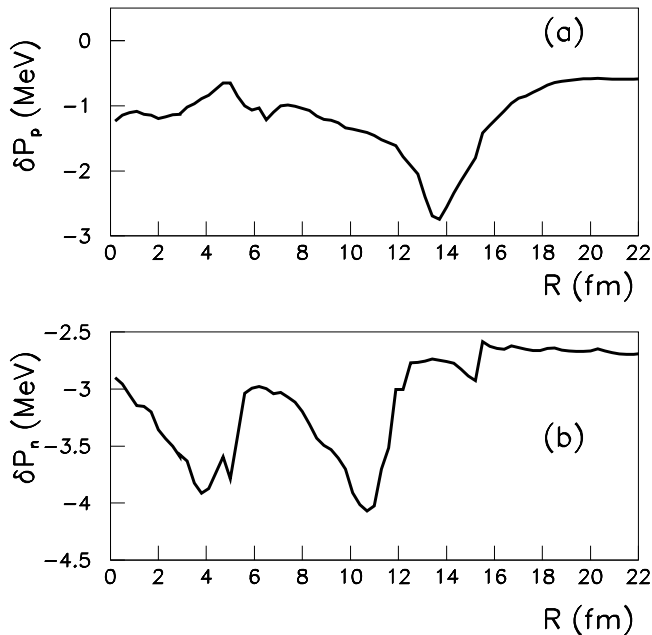


FIG. 9. Pairing correction δP for proton (a) and neutron (b) computed with a state dependent pairing interaction G_{ij} .

α $1s_{1/2}$ state crosses the Fermi energy of the whole system, as displayed in Fig. 3. A structure can be observed also in the case of the neutron pairing corrections δP_n . Close to $R \approx 15$ fm, a rapid fluctuation is produced. This fluctuation corresponds exactly to the moment in which the pairing gaps of the states that are located in the α nucleus become zero, as it can be seen in the Fig. 6 (a). A peak can be also observed in Fig. 9 (b) at $R \approx 8$ fm. This peak reflects that a low density of states is realized around the Fermi energy, as exhibited in Fig. 4.

For comparison, the pairing corrections space are represented in Fig. 10 with the constant interaction G approach. The structure of the pairing corrections resemble to that given by the state dependent pairing interactions method. However, the fluctuations at $R \approx 15$ fm obtained for neutron are missing.

CONCLUSION

The alpha decay was treated as a superasymmetric fission process with particular emphasis on the scission configuration. The pairing interaction was taken into account through the DDDI approach in terms of the two center shell model. The pairing gaps of the single particle states pertaining to the nascent alpha particle reach very large values close to scission. These values of the pairing gaps certainly suppress the quasiparticle excitation probabilities. So, the alpha particle forms a strong bound cluster when escaping from the parent nucleus. We have

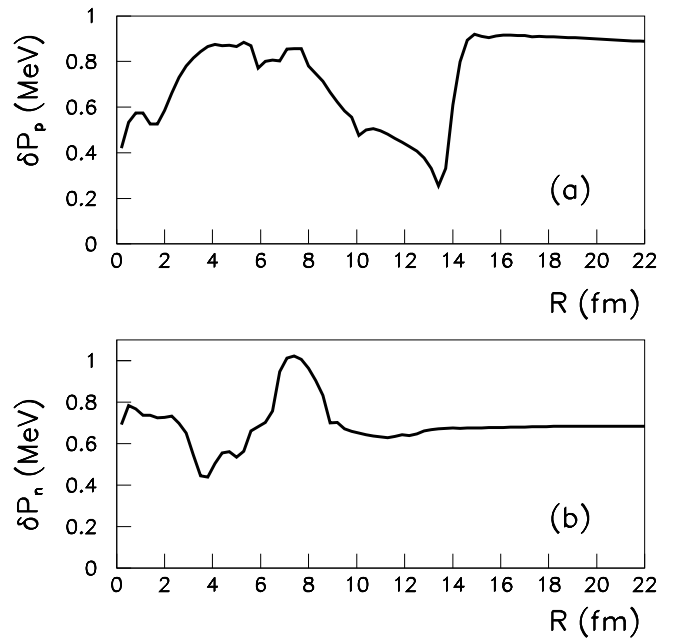


FIG. 10. Pairing correction δP for proton (a) and neutron (b) computed with a constant value of the interaction G .

a mechanism in which the α particle can be considered preformed on the surface of the daughter nucleus. When the overlaps between the wave functions that pertain to different fragments vanish, the pairing gaps of the alpha particle become zero. In the same time, the Fermi energy of the daughter nucleus reaches the value evaluated for the compound nuclear system. The projection of particle numbers was obtained in a natural way.

Many models invoke a preformation of the alpha particle in the parent nucleus in order to penetrate an Coulomb external barrier [38–41]. Such preformations are invoked also for ternary fission [42]. The preformation is proportional to the square overlaps between the ground state wave functions of the parent and the anti-symmetric product between the wave functions of the nascent fragments in different configurations after the scission [43, 44]. Our calculations show that when the nuclear shape parametrization describes very asymmetric systems, the nuclear matter builds a very bound cluster consisting of two protons and two neutrons on its surface. This cluster survives in the mean field created by the remaining nucleons. It was also assessed, at least formally, that the preformation of an emitted particle and its barrier penetrability between the ground state and the scission point are quantities with the same significance [45, 46]. This equivalence gives a support in the attempt to investigate the α decay process using fission theories in order to understand the mechanism of its formation. The DDDI formalism in conjunction with the two center shell model can offer a valuable tool for the investigation

of scission properties of nuclear disintegration.

Acknowledgements

The author is indebted to Krzysztof Pomorski for giving notice of the subject and for illuminating discussions. This work was supported by CNCS-UEFISCDI, Project No. PN-II-ID-PCE-2011-3-0068.

-
- [1] W. Younes, and D. Gogny, Phys. Rev. Lett. **107**, 132501 (2011).
 - [2] W. Warda, and J.L. Egido, Phys. Rev. C **86**, 014322 (2012).
 - [3] C. Simenel, and A.S. Umar, Physical Review C **89**, 031601(R) (2014).
 - [4] B.N. Lu, E.-G. Zhao, and S.-G. Zhou, Phys. Rev. C **85**, 011301 (2012).
 - [5] A. Sandulescu, M. Mirea, and D.S. Delion EPL **101**, 62001 (2013).
 - [6] M. Mirea, Physical Review C **78**, 044618 (2008).
 - [7] J.R. Nix, Ann. Rev. Nucl. Sci. **22**, 65 (1972).
 - [8] W.J. Swiatecki, and S. Bjornholm, Phys. Rep. **4**, 325 (1972).
 - [9] V.Yu. Denisov, Phys. Rev. C **89**, 044604 (2014).
 - [10] P. Moller, J.R. Nix, W.D. Myer, and W.J. Swiatecki, Atom. Data Nucl. Data Tabl. **59**, 185 (1995).
 - [11] M. Brack, J. Damgaard, A.S. Jensen, H.C. Pauli, V.M. Strutinsky, and C.Y. Wong, Rev. Mod. Phys. **44**, 320 (1972).
 - [12] K. Pomorski, and F. Ivanyuk, Int. J. Mod. Phys. E **18**, 900 (2009).
 - [13] W.D. Myers and, W.J. Swiatecki, Nucl. Phys. A **81**, 1 (1966).
 - [14] B. Nerlo Pomorska and, K. Pomorski, Int. J. Mod. Phys. E **16**, 328 (2007).
 - [15] M. Mirea, Phys. Rev. C **54**, 302 (1996).
 - [16] M. Mirea, Nucl. Phys. A **780**, 13 (2006).
 - [17] J. Maruhn, and W. Greiner, Z. Phys. **251**, 431 (1972).
 - [18] L.-S. Geng, J. Meng, and T. Hiroshi, Chin. Phys. Lett. **24**, 1865 (2007).
 - [19] A. Diaz-Torres, and W. Scheid, Nucl. Phys. A **757**, 373 (2005).
 - [20] A. Diaz-Torres, Phys. Rev. Lett. **101**, 122501 (2008).
 - [21] V.A. Nesterov, Phys. At. Nucl. **76**, 577 (2013).
 - [22] Q. Sun, D.-H. Shangguan, and J.-D. Bao, Chin. Phys. C **37**, 014102 (2013).
 - [23] H. Hassanabadi, E. Maghsoodi, and S. Zarrinkamar, Few-Body Syst. **53**, 271 (2012).
 - [24] A. Sandulescu, and M. Mirea, Eur. Phys. J. A **50**, 110 (2014).
 - [25] A. Sandulescu, and M. Mirea, Rom. Rep. Phys. **65**, 688 (2013).
 - [26] M. Mirea, Phys. Rev. C **63**, 034603 (2001).
 - [27] M. Mirea, Rom. J. Phys. **60**, in print (2015).
 - [28] M. Mirea, Physical Review C **83**, 054608 (2011).
 - [29] M. Mirea, Physics Letters B **717**, 252 (2012).
 - [30] M. Mirea, Physical Review C **89**, 034623 (2014).
 - [31] R.R. Chasman, Phys. Rev. C **14**, 1935 (1976).
 - [32] J. Dobaczewski, W. Nazarewicz, T.R. Werner, J.F. Berger, C.R. Chinn, and J. Decharge, Phys. Rev. C **53**, 2809 (1996).
 - [33] M. Bender, K. Rutz, P.-G. Reinhard, and J.A. Maruhn, Eur. Phys. J. A **8**, 59 (2000).
 - [34] S. Yoshida, and H. Sagawa, Phys. Rev. C **77**, 054308 (2008).
 - [35] N. Tajima, P. Bonche, H. Flocard, P.-H. Heenen, and M.S. Weiss, Nucl. Phys. A **551**, 434 (1993).
 - [36] M. Wang, G. Audi, A.H. Wapstra, F.G. Kondev, M. MacCormick, X. Xu, and B. Pfeiffer, Chin. Phys. C **36**, 1603 (2012).
 - [37] P. Moller, J.R. Nix, and K.-L. Kratz, Atom. Data. Nucl. Data. Tabl. **66**, 131 (1997).
 - [38] M. Avrigeanu, A.C. Obreja, F.L. Roman, V. Avrigeanu, and W. von Oertzen, At. Data Nucl. Data Tabl. **95**, 501 (2009).
 - [39] A.I. Budaca, and I. Silisteanu, Physical Review C **88**, 044618 (2013).
 - [40] K.P. Santhosh, J.G. Joseph, B. Priyanka, and S. Sahadevan, J. Phys. G **38**, 075101 (2011).
 - [41] R.G. Lovas, R.J. Liotta, A. Insolia, K. Varga, and D.S. Delion, Phys. Rep. **294**, 265 (1998).
 - [42] N. Carjan, A. Sandulescu, and V. V. Pashkevich, Phys. Rev. C **11**, 782 (1975).
 - [43] H. J. Mang, Phys. Rev. **119**, 1069 (1960).
 - [44] A. Sandulescu, Nucl. Phys. **37**, 332 (1962).
 - [45] D. N. Poenaru and W. Greiner, J. Phys. G **17**, S443 (1991).
 - [46] A. Zdeb, M. Warda, and K. Pomorski, Phys. Rev. C **87**, 024308 (2013).